Electronic Supplementary Information

Experimental Section

Materials: Sodium nitrate ($NaNO_3$, 99.0%), sodium nitrite ($NaNO_2$, 99.0%), ammonium chloride (NH_4Cl), sodium hydroxide (NaOH), sodium salicylate ($C_7H_5NaO_3$), salicylic acid ($C_7H_6O_3$), trisodium citrate dihydrate ($C_6H_5Na_3O_7 \cdot 2H_2O$), *p*-dimethylaminobenzaldehyde ($C_9H_{11}NO$), sodium nitroferricyanide dihydrate ($C_5FeN_6Na_2O \cdot H_2O$), 7,7,8,8-tetracyanoquinodimethane ($C_{12}H_4N_4$), sulfamic acid solution (H3NO3S), sodium hypochlorite solution (NaClO), $Na^{15}NO_3$, deuterium oxide (D_2O), acetonitrile (C_2H_3N), tetrabutylammonium perchlorate ($C_{16}H_{36}ClNO_4$), cobalt nitrate ($Co(NO_3)_2 \cdot 6H_2O$) and cobalt perchlorate ($Co(ClO_4)_2 \cdot 6H_2O$) were purchased from Aladdin Ltd. (Shanghai, China). Sulfuric acid (H_2SO_4), hydrogen peroxide (H_2O_2), hydrochloric acid (HCl), phosphoric acid (H_3PO_4), hydrazine monohydrate ($N_2H_4 \cdot H_2O$) and ethylalcohol (C_2H_5OH) were bought from Beijing Chemical Corporation. (China). chemical Ltd. in Chengdu. Graphite paper (GP) was provided by Hongshan District, Wuhan Instrument Surgical Instruments business. All reagents used in this work were analytical grade without further purification.

Preparation of CoO@NCNT/GP: CoO@NCNT/GP was synthesized by electrodeposition with annealing treatment.[1] Typically, 1.36 g tetrabutylammonium perchlorate ($C_{16}H_{36}ClNO_4$), 14.64 mg cobalt perchlorate ($Co(ClO_4)_2 \cdot 6H_2O$) and 16.32 mg 7,7,8,8-tetracyanoquinodimethane ($C_{12}H_4N_4$) were dissolved into 40 mL acetonitrile to form a homogeneous electrolyte. The GP (1 cm × 1.5 cm) was repeatedly wiped with alcohol before electrodeposition. The potentiostatic electrodeposition were performed with a CHI 760E potentiostat (CH Instruments, China) in a standard three-electrode setup with the GP as the working electrode, a graphite rod as the counter electrode, the Ag/AgCl electrode as the reference electrode. After constant-potential operation at –0.2 V vs. Ag/AgCl for 15 min, the precursor was formed. The CoO@NCNT/GP was obtained by calcining the precursor from room temperature to 400 °C with an increasing rate of 2 °C min^{-1} and then kept for 1 h under the Ar

atmosphere.

Preparation of CoO/GP: For preparing CoO/GP counterpart, we firstly synthesized $Co(OH)_2$. Typically, 0.1 M $Co(NO_3)_2 \cdot 6H_2O$ solution was used as electrolyte and the $Co(OH)_2$ were electrodeposited on GP (1 cm × 1.5 cm) under a constant potential of −1.0 V vs Ag/AgCl for 15 min. Then, the $Co(OH)_2$/GP was calcined at 200 °C with the increasing rate of 2 °C min^{-1} and kept for 2 h in Ar atmosphere to obtain CoO/GP.

Characterizations: X-ray diffraction (XRD) data was recorded by a LabX XRD-6100 X-ray diffractometer. Scanning electron microscopy (SEM) and energy-dispersive X-ray (EDX) elemental mapping images were acquired using GeminiSEM 300 (ZEISS, Germany) scanning electron microscope. Transmission electron microscopy (TEM) and high-resolution TEM (HRTEM) images were obtained from FEI Tecnai F20 transmission electron microscopy operated at an accelerating voltage of 200 kV. X-ray photoelectron spectroscopy (XPS) data was collected on an EscaLab Xi+ X-ray photoelectron spectrometer using Al as the exciting source. The absorbance data was measured on SHIMADZU UV-1800 Ultraviolet-visible (UV-Vis) spectrophotometer. H_2 were determined by GC with SHIMADZU GC-2014 gas chromatograph. A GC run was initiated per 1200 s. Argon (99.999%) was used as the carrier gas. A flame ionization detector with a thermal conductivity detector was used to quantify hydrogen and nitrogen. The electrolyzer outlet was introduced into a condenser before being vented directly into the gas sampling loop of the gas chromatograph.

Electrochemical measurements: All electrochemical tests were carried using a CHI 760E electrochemical potentiostat in an H-type cell separated by a nafion 117 membrane under an Ar-saturated atmosphere with continuous stirring of 250 rpm. The free-standing CoO@NCNT/GP (geometric area: 0.25 cm^{-2}), Hg/HgO and Pt plate were served as the working electrode, reference electrode and counter electrode, respectively. Before test, the nafion membrane was protonated by boiling in H_2O_2 (5%), 0.5 M H_2SO_4 and ultrapure water at 80 °C for 1 h one by one. 0.1 M NaOH solution was adopted as the electrolyte and extra 0.1 M NO_3^- was added as the reactants. All potentials were recorded to reversible hydrogen electrode (RHE) with the following equation: E (RHE)

= E (Hg/HgO) + (0.098 + 0.0591 × pH) V. Presented current density and NH_3 yields was normalized to the geometric surface area.

Determination of NH_3: We adopt indophenol blue method to quantify the concentration of produced NH_3.[2] The electrolytes after 2-h electrolysis were diluted 40 times due to the large concentration of produced NH_3. In detail, 2 mL of coloring solution (1 M NaOH containing 5 wt% salicylic acid and 5 wt% sodium citrate), 1 mL of the oxidizing solution (0.05 M sodium hypochlorite solution) and 200 uL catalyst solution (1 wt% sodium nitroferricyanide (III) dehydrate) were added slowly to the 2 mL diluted electrolyte one by one. The UV-Vis absorption spectra were performed at λ = 665 nm after the mixed solution standing for 2 h in the dark. The concentration-absorbance curve was calibrated by a serious of standard NH_4Cl solutions with different concentration. The fitting curve ($y = 0.39414x + 0.04382$, $R^2 = 0.9999$) shows good linear relation of absorbance value with NH_3 concentration.

Determination of NO_2^-: Griess method was adopt to quantify the concentration of NO_2^-.[3] The electrolytes were diluted 20 times. In brief, sulfonamide (1.0 g), H_3PO_4 (2.94 mL), N-(1-naphthyl)-ethylenediamine dihydrochloride (0.1 g), and deionized water (50 mL) was mixed as a color reagent. Then, 1 mL color reagent and 2 mL H_2O was added into 1 mL electrolyte after 2-h electrolysis. The absorbance was performed at a wavelength of 540 nm after the mixture stand 10 min in dark. The fitting curve ($y = 0.2211x + 0.03857$, $R^2 = 0.9998$) shows good linear relation of absorbance value with NO_2^- concentration.

Determination of N_2H_4: The Watt and Chrisp method was adopted to detect the N_2H_4 in the electrolyte.[4] In detail, $C_9H_{11}NO$ (5.99 g), HCl (30 ml) and C_2H_5OH (300mL) was mixed to form a uniform solution used as a color reagent. Then, 1 mL color reagent was added into 1 mL electrolyte after 2 h electrolysis. The absorbance was performed at a wavelength of 455 nm after the mixture stand 20 min in dark. The fitting curve ($y = 0.8465x + 0.1001$, $R^2 = 0.998$) shows good linear relation of absorbance value with N_2H_4 concentration.

Determination of NO_3^-: The electrolytes were diluted to the detection range. In brief,

0.1 mL 1 M HCl and 0.01 mL 0.8 wt% sulfamic acid solution were added into 5 mL diluted electrolyte. The absorption spectrum was measured using a UV-Vis spectrophotometer and the absorption intensities at a wavelength of 220 nm and 275 nm were recorded. The final absorbance value was calculated by this equation: $A = A_{220nm} - 2A_{275nm}$. The calibration curve can be obtained through different concentrations of $NaNO_3$ solutions and the corresponding absorbance. The fitting curve ($y = 0.05425x + 0.00388$, $R^2 = 0.999$) shows good linear relation of absorbance value with NO_3^- concentration.

$^{15}N_2$ isotope labeling experiments: The ^{15}N isotopic labeling experiment was conducted to confirm the N source of produced NH_3. After electrolysis in Ar-saturated 0.1 M NaOH with 0.1 M $^{15}NO_3^-$ at –0.6 V for 2 h, the pH of the obtained electrolyte was adjusted to be 2 with a 0.5 M H_2SO_4 solution. Then, 1 mL of electrolyte, 0.2 mL of DMSO and 0.2 mL of D_2O were added into the NMR tube for further NMR detection. The method for detecting the $^{14}NH_3$ is similar to this method except using the $^{14}NO_3^-$ as the reactants.

Determination of FE, NH_3 yield and selectivity:

$FE = n \times F \times C \times V / (M \times Q) \times 100\%$

$Yield = C \times V / (17 \times t \times A)$

$Selectivity = [NH_3] / \Delta[NO_3^-] \times 100\%$

Where n represent the number of electrons transferred for NO_3RR (the reduction of NO_3^- to NH_3 consumes 8 electrons), F is the Faraday constant (96485 C mol^{-1}), C is the concentration of produced NH_3 calculated by fitting curves, V is the volume of cathodic reaction electrolyte (40 mL), M is the relative molecular mass of NH_3, Q is the total quantity of applied electricity, t is the reduction time (2 h), and A is the geometric area of working electrode (0.25cm^{-2}). $\Delta[NO_3^-]$ is the concentration difference of NO_3^- before and after electrolysis.

Computational details:

First-principles calculations were performed by using the Vienna Ab initio Simulation Package (VASP)[5-8] to investigate the NO_3RR process on CoO surface. The valence-

core electrons interactions were treated by Projector Augmented Wave (PAW)[9] potentials and the electron exchange correlation interactions were described by the generalized gradient approximation (GGA) with the Perdew-Burke-Ernzerhof (PBE)[10] functional. Considered long-range interaction at the interface, Van der Waals interactions were considered using DFT-D3 correlation.[11] To avoid interaction come from other slabs, a vacuum of 20 Å was added along z direction. The convergence criterion of geometry relaxation was set to 0.03 eV•Å^{-1} in force on each atom. The energy cutoff for plane wave-basis was set to 500 eV. The K points were sampled with 3×3×1 by Monkhorst-Pack method.[12]

Gibbs free energy change (ΔG) was evaluated based on the computational hydrogen electrode (CHE) model, which takes one-half of the chemical potential of gaseous hydrogen under standard conditions as the free energy of the proton-electron pairs. ΔG were calculated by the following equation[13]:

$$\Delta G = \Delta E + \Delta E_{ZPE} - T\Delta S + neU$$

where ΔE, ΔE_{ZPE}, ΔS are the reaction energy from DFT calculation, the correction of zero-point energy and the change of simulated entropy, respectively. T is the temperature (T = 300 K). *n* and U are the number of transferred electrons and applied potential respectively.

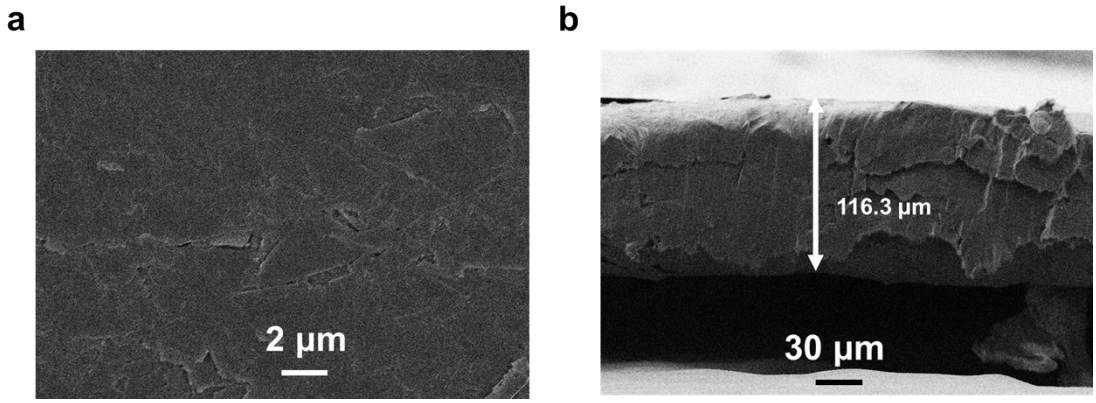

Fig. S1. (a) Top-view and (b) side-view SEM images of bare GP.

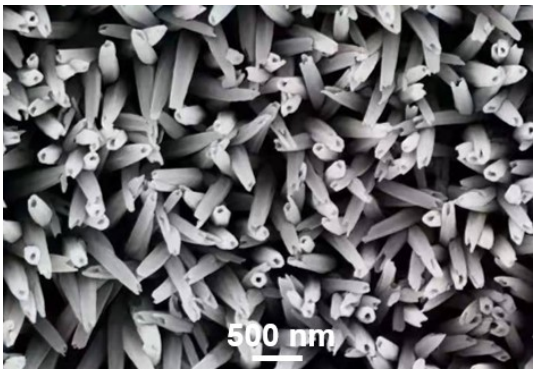

Fig. S2. SEM image of the precursor of CoO@NCNT/GP.

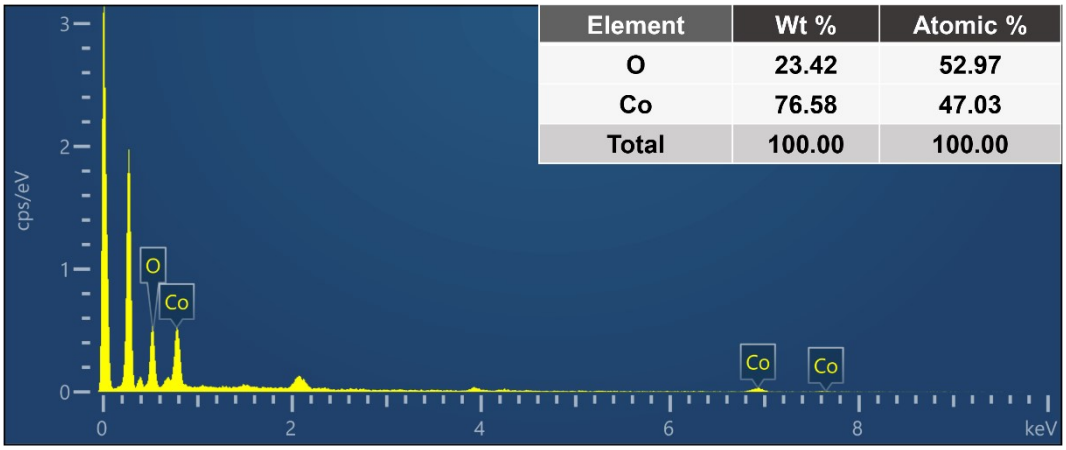

Fig. S3. EDX spectrum of CoO@NCNT/GP.

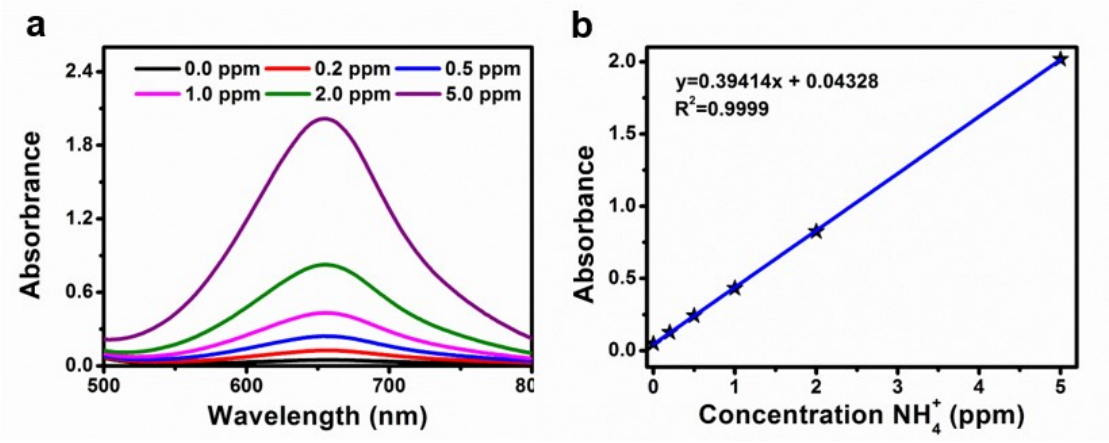

Fig. S4. (a) UV-Vis absorption spectra of different concentrations of NH_3 stained with indophenol blue method. (b) Calibration curve used to calculation of NH_3 concentration.

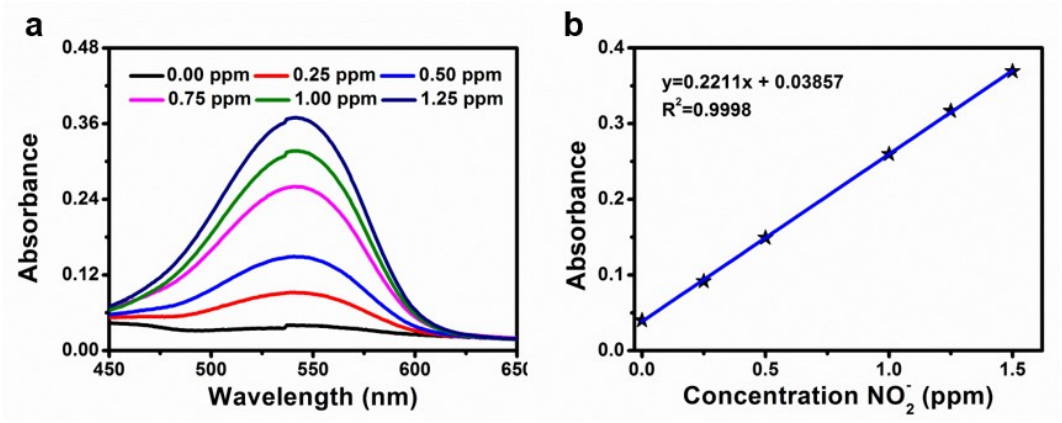

Fig. S5. (a) UV-Vis absorption spectra of different concentrations of NO_2^- using Griess method. (b) Calibration curve used to calculation of NO_2^- concentration.

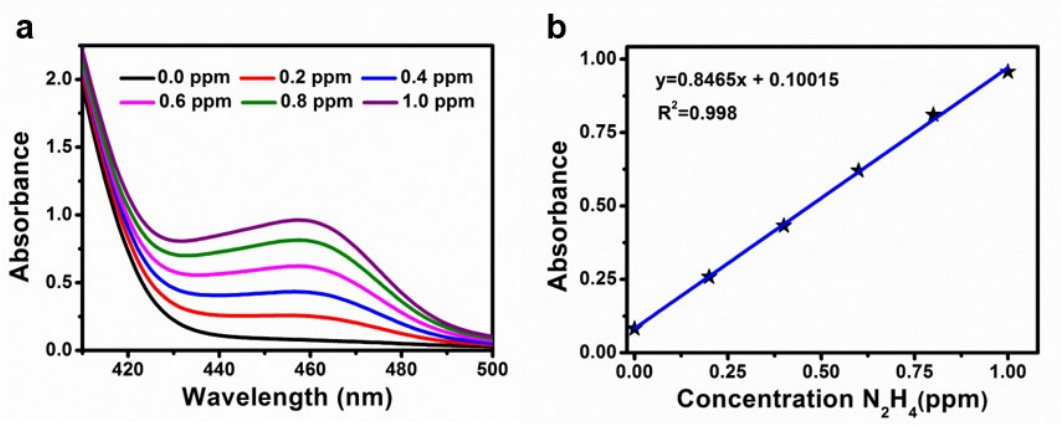

Fig. S6. (a) UV-Vis absorption spectra of different concentrations of N_2H_4 by Watt and Chrisp method. (b) Calibration curve used to calculation of N_2H_4 concentration.

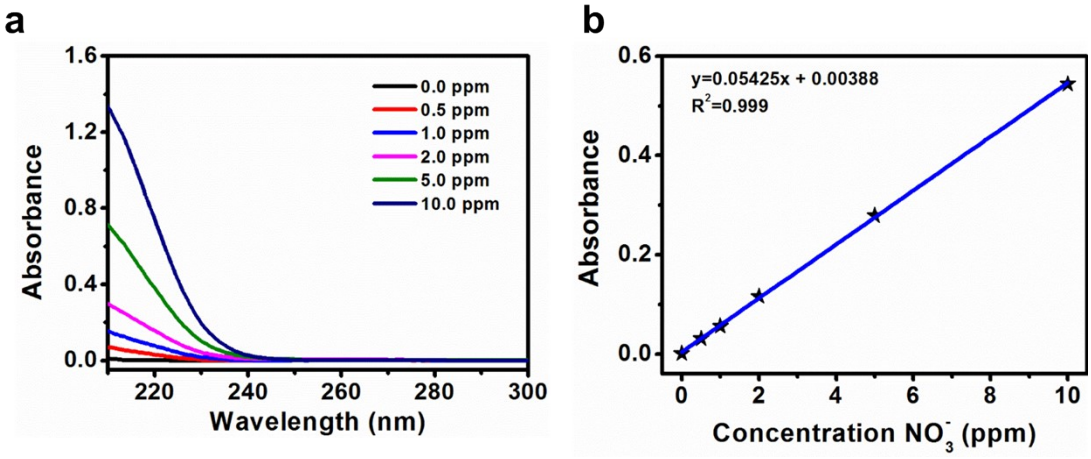

Fig. S7. (a) UV-Vis absorption spectra of different concentrations of NO_3^-. (b) Calibration curve used for calculation of NO_3^- concentration.

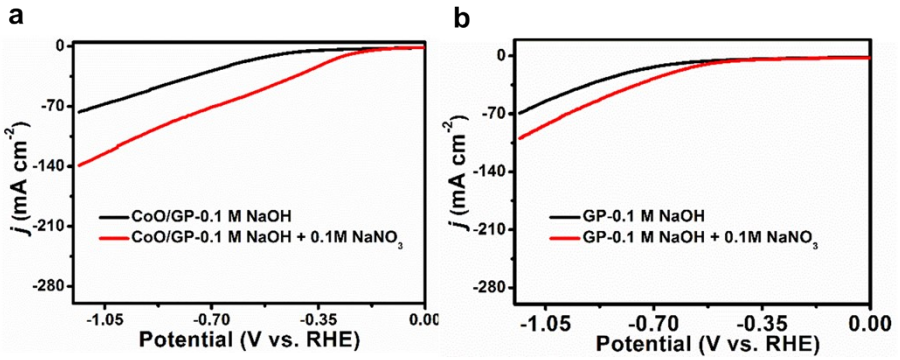

Fig. S8. LSV curves of (a) CoO/GP and (b) bare GP in 0.1 M NaOH solution with and without NO_3^-.

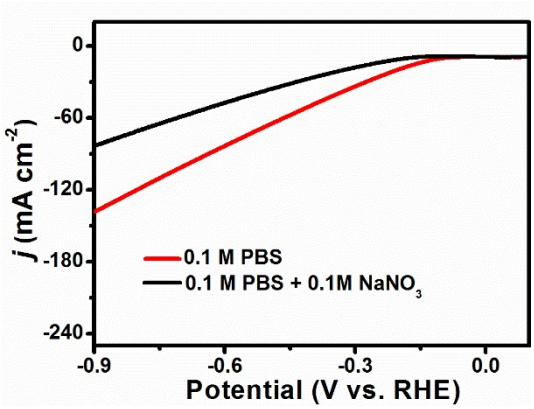

Fig. S9. LSV curves of CoO@NCNT/GP in 0.1 M PBS with and without NO_3^-.

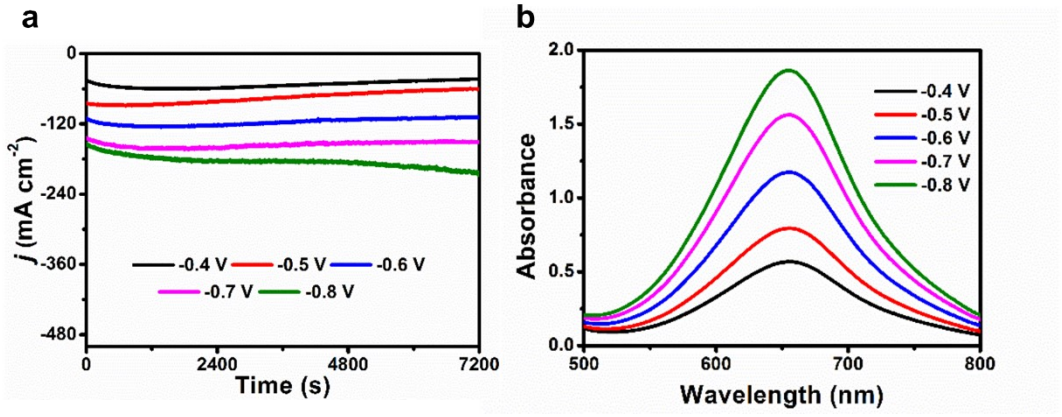

Fig. S10. (a) Chronoamperometry curves and (b) UV-Vis absorption spectra for CoO@NCNT/GP at different potentials in 0.1 M NaOH with 0.1 M NO_3^-.

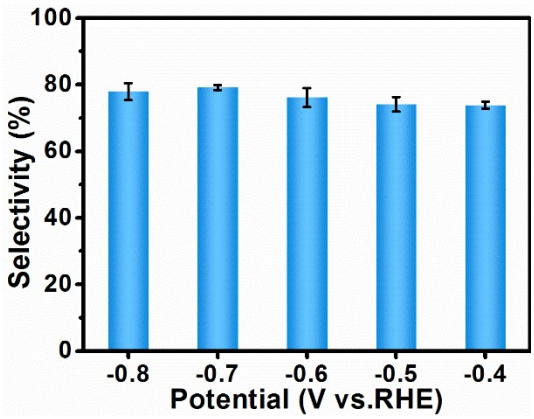

Fig. S11. Selectivity for NH_3 at different potentials.

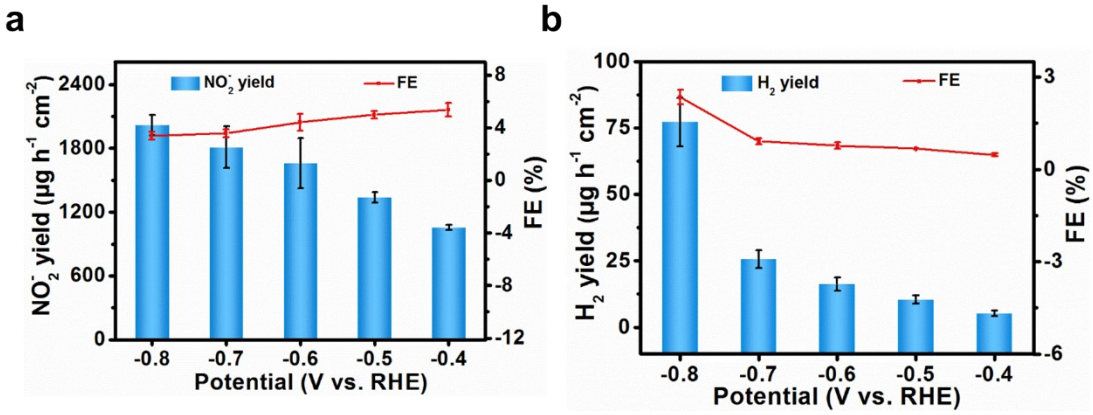

Fig. S12. FEs and yields of (a) NO_2^- and (b) H_2 at different applied potentials.

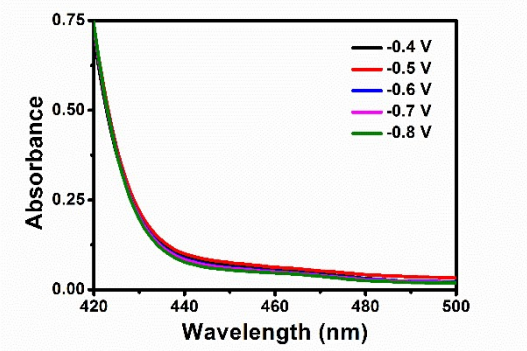

Fig. S13. UV-Vis absorption spectra of produced N_2H_4 at different potentials.

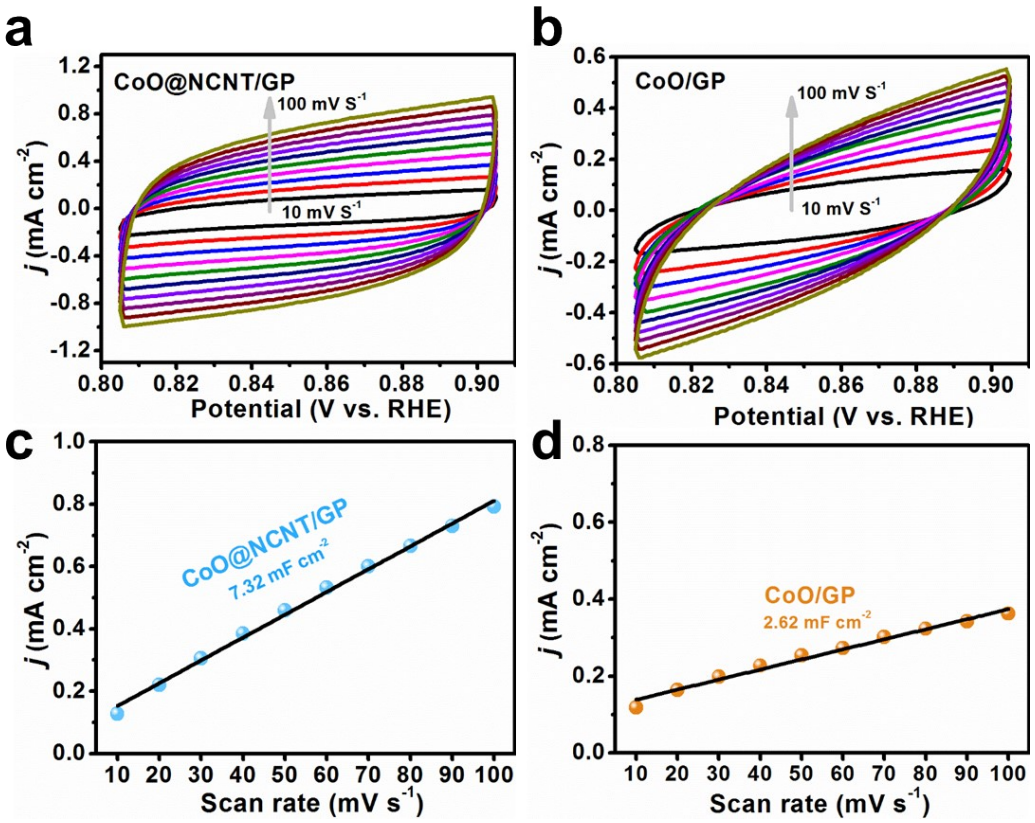

Fig. S14. CV curves for (a) CoO@NCNT/GP and (b) CoO /GP in the double layer region of 0.805-0.905 V at various scan rates. Capacitive current of (c) CoO@NCNT/GP and (d) CoO/GP as function of scan rate at 0.855 V.

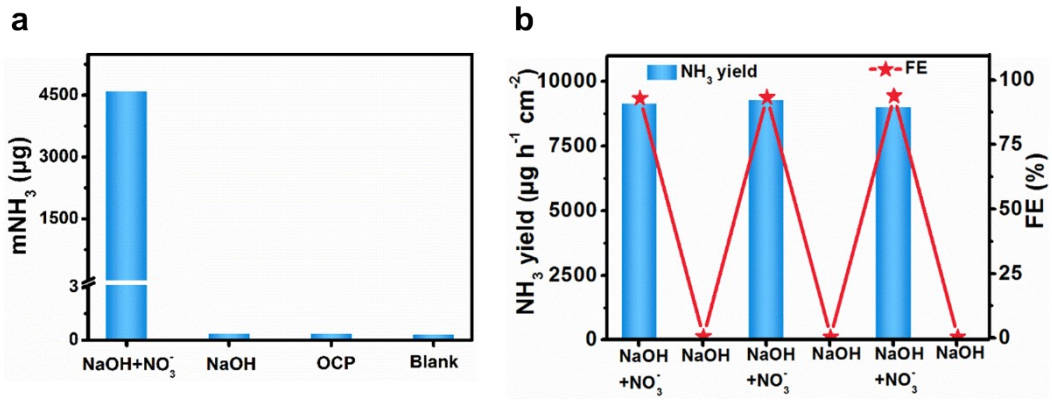

Fig. S15. (a) Amounts of produced NH_3 comparison under different conditions. (b) NH_3 yields and FEs during the alternating tests between 0.1 M NaOH with/without NO_3^- at −0.6 V.

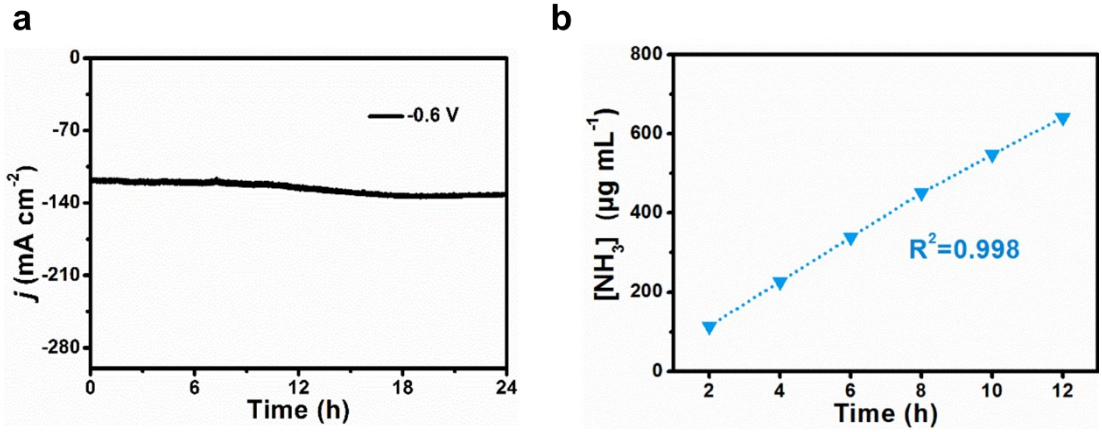

Fig. S16. (a) Chronoamperometry curve of 24 h electrolysis and (b) linear relationship between the produced NH_3 and the electrolysis time during the long-term test.

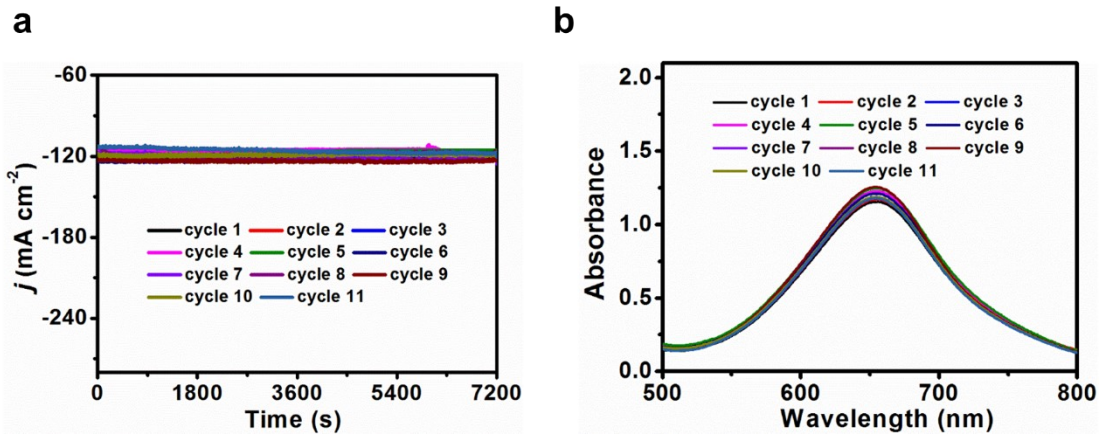

Fig. S17. (a) Chronoamperometry curves and (b) corresponding UV-Vis spectra of CoO@NCNT/GP during cycling tests at −0.6 V in 0.1 M NaOH with 0.1 M NO_3^-.

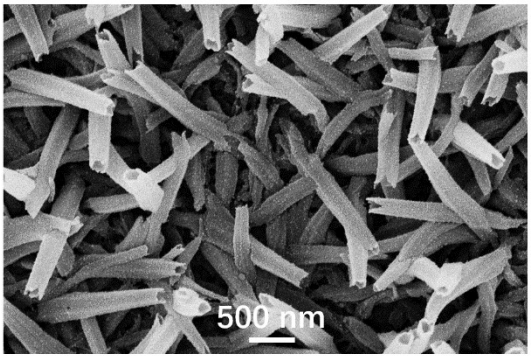

Fig. S18. SEM image for CoO@NCNT/GP after stability test.

Table S1. Comparison of electrocatalytic NO_3RR performance for CoO@NCNT/GP with other electrocatalysts under ambient conditions.

Catalyst	Electrolyte	NH_3 yield ($\mu g\ h^{-1}\ cm^{-2}$)	FE	Ref.
CoO@NCNT/GP	0.1 M NaOH (0.1 M NO_3^-)	9041.6 ± 370.7	93.8 ± 1.5 %	This work
Co/CoO NSA	0.1 M Na_2SO_4 (200 ppm NO_3^-)	3305	93.8 %	14
Co–P/TP	0.2 M Na_2SO_4 (200 ppm NO_3^-)	416.0 ± 7.2	93.6 ± 3.3 %	15
Fe SAC	0.1 M K_2SO_4 (0.5 M NO_3^-)	7820	75.0 %	16
Fe_3O_4/SS	0.1 M NaOH (0.1 M NO_3^-)	10145	91.6 %	17
Fe-PPy-SACs	0.1 M KOH (0.1 M NO_3^-)	2749	~100 %	18
$Cu_{50}Ni_{50}$	0.1 M KOH (0.1 M NO_3^-)	-	84.0 %	19
Cu_3P NA/CF	0.1 M PBS (0.1 M NO_3^-)	848	62.9 %	20
Cu/Cu_2O NWAs	0.5 M Na_2SO_4 (200 ppm NO_3^-)	4148	95.8 %	21
TiO_{2-x}	0.5 M Na_2SO_4 (400 ppm NO_3^-)	770	87.1%	22

References

1 C. Yang, H. Zhang, K. Yu, S. Xie, H. Tong, Y. Song, G. Shi, H. Gu, C. Chen and L Zhang, *ACS Appl. Energy Mater.*, 2020, **3**, 2010–2019.

2 D. Zhu, L. Zhang, R. E. Ruther and R. J. Hamers, *Nat. Mater.,* 2013, **12**, 836–841.

3 P. Li, Z. Jin, Z. Fang and G. Yu, *Energy Environ. Sci.*, 2021, **14**, 3522–3531.

4 G. W. Watt and J. D. Chrisp, *Anal. Chem.,* 1952, **24**, 2006–2008.

5 G. Kresse and J. Furthmüller, *Phys. Rev. B*, 1996, **54**, 11169.

6 G. Kresse and J. Furthmüller, J. *Comp. Mater. Sci.*, 1996, **6**, 15–50.

7 G. Kresse and J. Hafner, *Phys. Rev. B*, 1994, **49**, 14251–14269.

8 M. Segall, P. J. Lindan, M. a. Probert, C. J. Pickard, P. J. Hasnip, S. Clark and M. Payne, *J. Phys-Condens Mat.*, 2002, **14**, 2717.

9 P. E. Blöchl, *Phys. Rev. B*, 1994, **50**, 17953.

10 J. P. Perdew, J. A. Chevary, S. H. Vosko, K. A. Jackson, M. R. Pederson, D. J. Singh and C. Fiolhais, *Phys. Rev. B*, 1992, **46**, 6671.

11 S. Grimme, J. Antony, S. Ehrlich and H. A. Krieg, *J. Chem. Phys.*, 2010, **132**, 154104.

12 H. J. Monkhorst and J. D. Pack, *Phys. Rev. B*, 1976, **13**, 5188.

13 J. Norskov, J. Rossmeisl, A. Logadottir, L. Lindqvist, J. Kitchin, T. Bligaard, and H. Jonsson, *J. Phys. Chem. B*, 2004, **108**, 17886–17892.

14 Y. Wang, C. Liu, B. Zhang and Y. Yu, *Sci. China Mater.* 2020, **63**, 2530–2538.

15 Y. Yu, C. Wang, Y. Yu, Y. Wang and B. Zhang, *Sci. China Chem.,* 2020, **63**, 1469–1476.

16 X. Fu, X. Zhao, X. Hu, K. He, Y. Yu, T. Li, Q. Tu, X. Qian, Q. Yue, M. R. Wasielewski and Y. Kang, *Appl. Mater. Today*, 2020, **19**, 100620.

17 R. Jia, Y. Wang, C. Wang, Y. Ling, Y. Yu and B. Zhang, *ACS Catal.,* 2020, **10,** 3533–3540.

18 G. Chen, Y. Yuan, H. Jiang, S. Ren, L. Ding, L. Ma, T. Wu, J. Lu and H. Wang, *Nat. Energy,* 2020, **5**, 605–613.

19 Y. Wang, W. Zhou, R. Jia, Y. Yu and B. Zhang, *Angew. Chem., Int. Ed.,* 2020, **59**, 5350–5354.

20 Y. Huang, J. Long, Y. Wang, N. Meng, Y. Yu, S. Lu, J. Xiao and B. Zhang, *ACS Appl. Mater. Interfaces,* 2021, **13**, 54967–54973.

21 F. Lei, W. Xu, J. Yu, K. Li, J. Xie, P. Hao, G. Cui and B. Tang, *Chem. Eng. J.,* 2021, **426**, 131317.

22 D. Reyter, G. Chamoulaud, D. Bélanger and L. Roué, *J. Electroanal. Chem.,* 2006, **596**, 13–24.

23 Y. Wang, A. Xu, Z. Wang, L. Huang, J. Li, F. Li, J. Wicks, M. Luo, D. H. Nam, C. Tan, Y. Ding, J. Wu, Y. Lum, C. T. Dinh, D. Sinton, G. Zheng and E. H. Sargent, *J. Am. Chem. Soc.,* 2020, **142**, 5702–5708.